

Synchronization of weakly nonlinear oscillators with Huygens' coupling

Citation for published version (APA):

Pena Ramirez, J., Fey, R. H. B., & Nijmeijer, H. (2013). Synchronization of weakly nonlinear oscillators with Huygens' coupling. *Chaos*, 23(3), 033118-1/12. Article 033118. <https://doi.org/10.1063/1.4816360>

DOI:

[10.1063/1.4816360](https://doi.org/10.1063/1.4816360)

Document status and date:

Published: 01/01/2013

Document Version:

Accepted manuscript including changes made at the peer-review stage

Please check the document version of this publication:

- A submitted manuscript is the version of the article upon submission and before peer-review. There can be important differences between the submitted version and the official published version of record. People interested in the research are advised to contact the author for the final version of the publication, or visit the DOI to the publisher's website.
- The final author version and the galley proof are versions of the publication after peer review.
- The final published version features the final layout of the paper including the volume, issue and page numbers.

[Link to publication](#)

General rights

Copyright and moral rights for the publications made accessible in the public portal are retained by the authors and/or other copyright owners and it is a condition of accessing publications that users recognise and abide by the legal requirements associated with these rights.

- Users may download and print one copy of any publication from the public portal for the purpose of private study or research.
- You may not further distribute the material or use it for any profit-making activity or commercial gain
- You may freely distribute the URL identifying the publication in the public portal.

If the publication is distributed under the terms of Article 25fa of the Dutch Copyright Act, indicated by the "Taverne" license above, please follow below link for the End User Agreement:

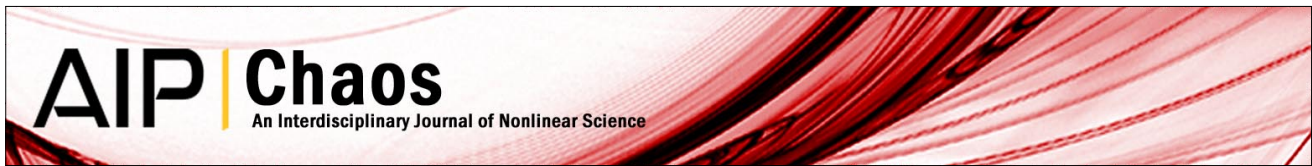
www.tue.nl/taverne

Take down policy

If you believe that this document breaches copyright please contact us at:

openaccess@tue.nl

providing details and we will investigate your claim.



Synchronization of weakly nonlinear oscillators with Huygens' coupling

J. Pena Ramirez, Rob H. B. Fey, and H. Nijmeijer

Citation: *Chaos* **23**, 033118 (2013); doi: 10.1063/1.4816360

View online: <http://dx.doi.org/10.1063/1.4816360>

View Table of Contents: <http://chaos.aip.org/resource/1/CHAOEH/v23/i3>

Published by the [AIP Publishing LLC](#).

Additional information on Chaos

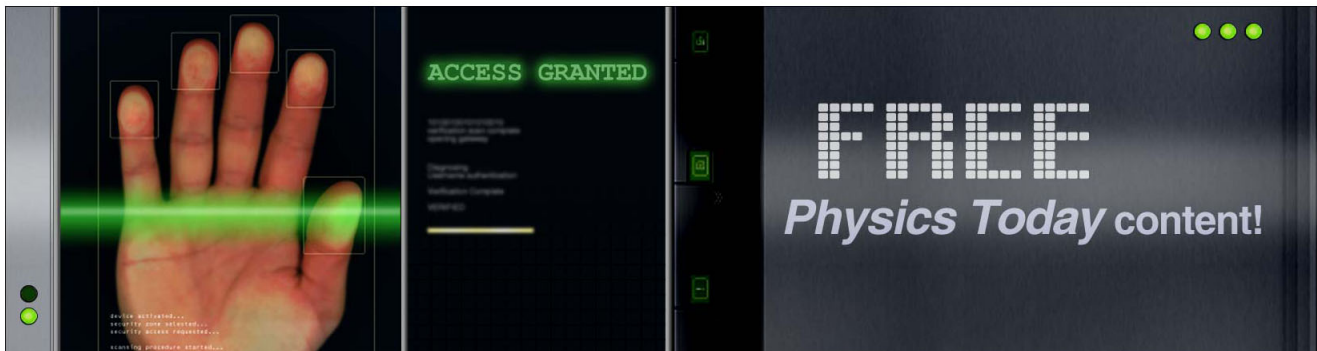
Journal Homepage: <http://chaos.aip.org/>

Journal Information: http://chaos.aip.org/about/about_the_journal

Top downloads: http://chaos.aip.org/features/most_downloaded

Information for Authors: <http://chaos.aip.org/authors>

ADVERTISEMENT



Synchronization of weakly nonlinear oscillators with Huygens' coupling

J. Pena Ramirez,^{a)} Rob H. B. Fey,^{b)} and H. Nijmeijer^{c)}

Department of Mechanical Engineering, Eindhoven University of Technology, P.O. Box 513,
5600 MB Eindhoven, The Netherlands

(Received 20 April 2013; accepted 9 July 2013; published online 30 July 2013)

In this paper, the occurrence of synchronization in pairs of weakly nonlinear self-sustained oscillators that interact via Huygens' coupling, i.e., a suspended rigid bar, is treated. In the analysis, a generalized version of the classical Huygens' experiment of synchronization of two coupled pendulum clocks is considered, in which the clocks are replaced by arbitrary self-sustained oscillators. Sufficient conditions for the existence and stability of synchronous solutions in the coupled system are derived by using the Poincaré method. The obtained results are supported by computer simulations and experiments conducted on a dedicated experimental platform. It is demonstrated that the mass of the coupling bar is an important parameter with respect to the limit synchronous behaviour in the oscillators. © 2013 AIP Publishing LLC.

[<http://dx.doi.org/10.1063/1.4816360>]

Probably, the earliest writing on inanimate synchronization is due to the Dutch scientist Christiaan Huygens (1629–1695), who discovered that two pendulum clocks hanging from a common support show synchronized behaviour. Since then, Huygens' synchronization has drawn the attention of many researchers.^{3,7,20,21,28,33} However, a complete understanding of this phenomenon is still missing. Consequently, the present contribution aims to provide new insights into the intriguing synchronization phenomenon discovered by Huygens. In particular, the following questions are addressed: given the Huygens system of coupled pendulum clocks, is it possible to replace the pendulum clocks by other types of second order nonlinear oscillators and still to observe the synchronized motion? Additionally, which is/are the key parameter(s) in the coupled system for the occurrence of in-phase, respectively, anti-phase, synchronization? These questions are answered by means of theoretical analysis, computer simulations, and experiments.

I. INTRODUCTION

Oscillatory motion is a ubiquitous form of motion in the universe. When the oscillatory motion of a system is influenced by the oscillations of (an)other oscillatory system(s), then the interacting systems may experience a striking phenomenon called *synchronization*. Synchronization, or as the Oxford advanced dictionary defines it, “agreement in time” or “happening at the same time,”¹ is one of the most deeply rooted and pervasive behaviours in nature. It extends from human beings to unconscious entities.^{25,29,30}

A natural question is: “under what conditions do a pair or group of oscillatory systems show synchronized behaviour?” The famous example by Christiaan Huygens of two pendulum clocks hanging from a suspended wooden bar, see

Figure 1(a), exhibiting anti-phase synchronized motion as he brought forward in his notebook⁶ addresses this question. Despite the lack of good modelling tools, Huygens did realize that there is a “medium,” “the coupling,” responsible for the synchronized motion, namely the bar, to which both pendula were attached. This coupling bar is, therefore, referred to as *Huygens' coupling*.

In this paper, the onset of synchronization in pairs of weakly nonlinear self-driven oscillators that interact via Huygens' coupling is investigated. In the analysis, a *generalized* version of the original Huygens system of pendulum clocks, see Figure 1(b), is considered. It is generalized in the sense that both pendulum clocks are replaced by two identical but arbitrary oscillators. The coupling bar supported by two chairs, i.e., the Huygens coupling, is modelled by a single degree of freedom (dof) suspended rigid bar, which is considered as the key element in the occurrence of synchronization. Moreover, it is assumed that the oscillators are subject to the following *limitations*:

- small damping,
- weak nonlinearities, and
- small coupling strength.

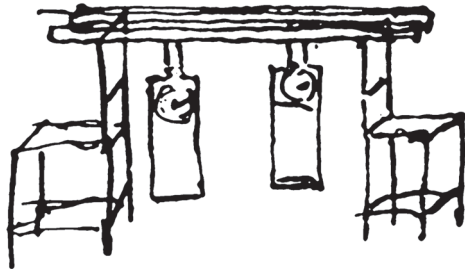
Here, small has to be understood in the sense that the value of the parameter (damping coefficient and/or coupling strength parameter) is much less than unity. The term weak indicates that the magnitude of the nonlinear terms is small when compared to the magnitude of the linear terms. In consequence, the dynamic behaviour of each nonlinear oscillator is close to a harmonic oscillator.

The aforementioned assumptions/limitations on the oscillators allow to analyze, to a large extent, the occurrence of synchronization by means of approximate methods of the theory of oscillations.^{2,4,8,10,32} For the present analysis, a result based on the Poincaré method is used in order to derive conditions, under which synchronous solutions in a pair of nonlinear oscillators with Huygens' coupling exist and are stable. In particular, it is shown that the mass of the coupling bar, which is directly associated with the coupling strength, is an important

^{a)}Electronic mail: j.pena@tue.nl

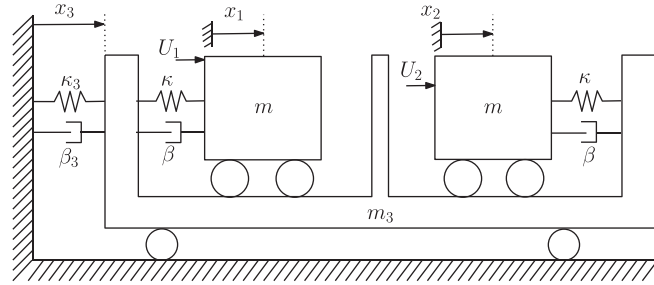
^{b)}Electronic mail: R.H.B.Fey@tue.nl

^{c)}Electronic mail: h.nijmeijer@tue.nl



(a) Original drawing of Huygens.

Reprinted from C. Huygens, *Oeuvres completes de Christiaan Huygens*, vol. 17, edited by M. Nijhoff (The Hague, 1932).



(b) Generalized version of Huygens' model.

FIG. 1. Huygens' original system of pendulum clocks and its generalized (and modern) version.

parameter with respect to the limit synchronized behaviour in the oscillators, namely in-phase or anti-phase synchronization.

Throughout the manuscript, the synchronization phenomenon is interpreted in the following manner. For the theoretical analysis while assuming identical oscillators, the strongest definition of synchronization is used: two oscillators are said to be synchronized if their frequencies and amplitudes are identical and their mutual phase difference is either 0 (in-phase synchronization) or π (anti-phase synchronization). For the experimental analysis, where there are unavoidable small mismatches between the oscillators, we use the concept of practical synchronization:¹¹ two oscillators are said to be practically synchronized if the difference in their amplitudes and frequencies is below a certain “small” threshold value and their mutual phase difference is “sufficiently close” to 0 (practical in-phase synchronization) or π (practical anti-phase synchronization).

This manuscript is organized as follows. First, in Sec. II the mathematical framework used is briefly described. Next, Sec. III presents an analysis of the synchronous behaviour occurring in a pair of nonlinear oscillators, driven by an energy-dependent term, which interact via Huygens' coupling. In Sec. IV, a similar analysis is performed for the case of nonlinear oscillators driven by a van der Pol term. Finally, in Sec. V, for both cases, it is experimentally demonstrated that the two nonlinear oscillators may synchronize in-phase or in anti-phase in a natural way via Huygens' coupling. The paper is concluded by a discussion of the obtained results.

II. PRELIMINARIES

Consider the dynamical system

$$\dot{x}_s = \sum_{j=1}^l a_{sj}x_j + \mu\Phi_s(x_1, \dots, x_l), \quad s = 1, \dots, l, \quad (1)$$

where a_{sj} are real constants and $\mu > 0$ is a “sufficiently small” real parameter.¹² The following assumption is made on system (1):

A-1: The functions $\Phi_s(x_1, \dots, x_l)$ are analytical functions in x_1, \dots, x_l , i.e., they can be expanded as a power series in x_1, \dots, x_l or they are polynomials.

When $\mu = 0$, system (1) can be written as a set of linear differential equations with constant coefficients, i.e.,

$$\dot{x} = Ax, \quad (2)$$

where $A \in \mathbb{R}^{l \times l}$ and $x = [x_1, \dots, x_l]^T$. For the matrix A , the following assumption is made:

A-2: The characteristic equation associated to matrix A has k ($0 < k \leq l$) purely imaginary roots of any multiplicity¹³ and the remaining roots are assumed to be either real or complex but with negative real part.

Then, by using a nonsingular linear transformation, system (1) can be transformed to the canonical form

$$\dot{y}_s = \lambda_s y_s + \mu f_s(y_1, \dots, y_l) \quad s = 1, \dots, l. \quad (3)$$

The *fundamental* or *generating* system, i.e., system (3) with $\mu = 0$ is

$$\dot{y}_s = \lambda_s y_s, \quad s = 1, \dots, l, \quad (4)$$

which has the solution

$$y_s^0 = \alpha_s e^{\lambda_s t}, \quad s = 1, \dots, l, \quad (5)$$

where $\alpha_s, s = 1, \dots, l$ are arbitrary parameters determining the amplitude of the solution.

A-3: In accordance with A-2, it is assumed that the *characteristic exponents* $\lambda_s, s = 1, \dots, l$ are categorized as follows:

$$\lambda_s = \begin{cases} in_s\omega, & s = 1, \dots, k, \\ -a_s + ib_s, & s = k + 1, \dots, l, \end{cases} \quad (6)$$

where i is the imaginary unit, i.e., $i = \sqrt{-1}$, $a_s > 0$, n_s is a positive or negative integer, $\omega = \frac{2\pi}{T}$ is the oscillation frequency associated to system (4) and T is the period. It will

also be assumed that only real solutions x_s of Eq. (1) are of interest (physical systems do not have complex solutions). Therefore, the characteristic exponents with purely imaginary part appear as complex conjugate pairs and likewise the functions f_s appear as complex conjugate pairs. This implies that k is a positive even number.

From the above assumption, it follows that system (4) will have periodic solutions of period T . Moreover, the asymptotic periodic solutions associated to Eq. (4) can be written as

$$y_s^0 = \begin{cases} \alpha_s e^{\lambda_s t} = \alpha_s e^{in_s \omega t} & s = 1, \dots, k, \\ 0 & s = k + 1, \dots, l. \end{cases} \quad (7)$$

The problem now is to determine the values of α_s , $s = 1, \dots, k$, such that (asymptotically) the periodic solutions of Eq. (3) reduce, for $\mu = 0$, to the generating solutions (7) of period T . Moreover, the periodic solutions of Eq. (3) will have a period different from T , i.e., $T^*(\mu) = T + \tau_c(\mu)$. Therefore, it is also necessary to determine the ‘‘correction’’ $\tau_c(\mu)$ of the period. The following result, which is due to Blekhnman,⁴ addresses these issues and also provides conditions for the existence and stability of periodic solutions in system (3).

Theorem 1. [Blekhnman⁵] *Periodic solutions with period $T^*(\mu) = T + \tau_c(\mu)$ for the autonomous system (3) becoming at $\mu = 0$ periodic (period T) solutions (7) of the fundamental system (4) can correspond only to such values of constants $\alpha_1, \dots, \alpha_{k-2}, \alpha_{k-1} = \alpha_k$, which satisfy equations*

$$R_s(\alpha_1, \dots, \alpha_k) = \alpha_k n_k P_s - \alpha_s n_s P_k = 0, \quad s = 1, \dots, k - 1, \quad (8)$$

where

$$P_s(\alpha_1, \dots, \alpha_k) = \int_0^T f_s(y_1^0, \dots, y_l^0) e^{-in_s \omega t} dt \quad (9)$$

$$= \int_0^T f_s(\alpha_1 e^{in_1 \omega t}, \dots, \alpha_k e^{in_k \omega t}, 0, \dots, 0) e^{-in_s \omega t} dt, \quad (10)$$

$s = 1, \dots, k.$

If for a certain set of constants $\alpha_1 = \alpha_1^*, \dots, \alpha_{k-2} = \alpha_{k-2}^*, \alpha_{k-1} = \alpha_k = \alpha_k^*$, which satisfy Eq. (8), the real parts of all roots χ of the following algebraic equation are negative¹⁴

$$\left| \frac{\partial R_s}{\partial \alpha_j} - \alpha_k n_k \delta_{sj} \chi \right| = 0, \quad s, j = 1, \dots, k - 1, \quad (11)$$

then, for sufficiently small μ , this set of constants will indeed correspond to a unique, analytically w.r.t. μ , stable periodic solution of Eq. (3) with period $T^*(\mu) = T + \tau_c(\mu)$. At $\mu = 0$, it becomes a periodic (period T) solution (7) of the fundamental system (4). If the real part of at least one root of Eq. (11) is positive, then the respective solution is unstable. With accuracy up to terms of order μ , the period correction $\tau_c(\mu)$ is determined by

$$\tau_c(\mu) = -\mu \frac{P_k(\alpha_1^*, \dots, \alpha_{k-2}^*, \alpha_k^*, \alpha_k^*)}{\lambda_k \alpha_k^*}. \quad (12)$$

The proof is sketched in Ref. 4 (in Russian) and in Ref. 23 (in English) and a recent application is presented in Ref. 7.

III. SYNCHRONIZATION OF OSCILLATORS DRIVEN BY AN ENERGY-DEPENDENT TERM

Consider the schematic model depicted in Figure 1(b), which can be seen as a simplified though generalized version of Huygens’ setup of pendulum clocks. In this model, the two pendulum clocks are now replaced by two (actuated) mass-spring-damper oscillators. The wooden bar supported by two chairs is substituted by a single dof suspended rigid bar. Clearly, in the generalized model, rotational angles are replaced by translational displacements. Furthermore, it comes natural to relate the control inputs U_i , $i = 1, 2$ to the escape-mechanisms (cf. Ref. 9) as used in the pendulum clocks.

The results presented in this section correspond to the case where the resupply of energy into the oscillators is provided by the energy-dependent term

$$U_i = -\vartheta(H_i - H^*)\dot{x}_i, \quad i = 1, 2, \quad (13)$$

where $\vartheta \in \mathbb{R}_+$ and $H^* = \frac{1}{2} \kappa x_{ref}^2$, which is a reference energy level with x_{ref} being a reference amplitude, and H_i is the Hamiltonian of the uncoupled and unforced oscillator i and is defined by

$$H_i = \frac{1}{2} m \dot{x}_i^2 + \frac{1}{2} \kappa x_i^2, \quad i = 1, 2. \quad (14)$$

Hence, the dynamic behaviour of the generalized Huygens system depicted in Figure 1(b) with inputs (13) is described by the set of equations

$$\ddot{x}_i = -\omega^2(x_i - x_3) - 2\zeta\omega(\dot{x}_i - \dot{x}_3) - \lambda(H_i - H^*)\dot{x}_i, \quad i = 1, 2, \quad (15)$$

$$\ddot{x}_3 = -\omega_3^2 x_3 - 2\zeta_3 \omega_3 \dot{x}_3 - \mu \sum_{i=1}^2 \ddot{x}_i, \quad (16)$$

where $x_i \in \mathbb{R}$, $i = 1, 2$, denotes the displacement of oscillator i and $x_3 \in \mathbb{R}$ denotes the displacement of the coupling bar, $\omega = \sqrt{\frac{\kappa}{m}}$, $\kappa \in \mathbb{R}_+$, $m \in \mathbb{R}_+$, $\zeta = \frac{\beta}{2\omega m}$, $\beta \in \mathbb{R}_+$ are the angular eigenfrequency, the stiffness, the mass, the dimensionless damping coefficient, and the damping constant of each oscillator, respectively. The angular eigenfrequency of the coupling bar is denoted by $\omega_3 = \sqrt{\frac{\kappa_3}{m_3}}$ and $\kappa_3 \in \mathbb{R}_+$, $m_3 \in \mathbb{R}_+$, $\zeta_3 = \frac{\beta_3}{2\omega_3 m_3}$, $\beta_3 \in \mathbb{R}_+$ are the stiffness, the mass, the dimensionless damping coefficient, and the damping constant of the free coupling bar, respectively. The dimensionless small parameter $0 < \mu = \frac{m}{m_3} \ll 1$ denotes the coupling strength and $\lambda = \frac{\vartheta}{m} \in \mathbb{R}_+$.

Rescaling the time by $\tau = \omega t$ yields system (15), (16) in the form

$$x_i'' = -(x_i - x_3) - p(x_i' - x_3') - \bar{\lambda}(ax_i'^2 + \kappa x_i^2 - \gamma)x_i', \quad i = 1, 2, \quad (17)$$

$$x_3'' = -qx_3 - sx_3' - \mu \sum_{i=1}^2 x_i'', \quad (18)$$

where the primes denote differentiation with respect to the dimensionless time τ , $p = 2\zeta$, $\bar{\lambda} = \frac{\lambda}{2\omega}$, $a = m\omega^2$, $\gamma = 2H^*$, $q = \frac{\omega_3^2}{\omega^2}$, and $s = \frac{2\zeta_3\omega_3}{\omega}$.

Furthermore, it is assumed that the damping in the oscillators is small, i.e., $p = \mu d$ and that the nonlinearity is small, i.e., $\bar{\lambda} = \mu\alpha$. These assumptions yield the system

$$x_i'' = -(x_i - x_3) - \mu(d(x_i' - x_3') - \alpha(ax_i'^2 + \kappa x_i^2 - \gamma)x_i'), \quad (19)$$

$$x_3'' = -qx_3 - sx_3' - \mu \sum_{i=1}^2 x_i'', \quad i = 1, 2. \quad (20)$$

After neglecting quadratic terms in μ , Eqs. (19) and (20) can be written in the form

$$x' = Ax + \mu\Phi(x), \quad (21)$$

with

$$A = \begin{bmatrix} 0 & 1 & 0 & 0 & 0 & 0 \\ -1 & 0 & 0 & 0 & 1 & 0 \\ 0 & 0 & 0 & 1 & 0 & 0 \\ 0 & 0 & -1 & 0 & 1 & 0 \\ 0 & 0 & 0 & 0 & 0 & 1 \\ 0 & 0 & 0 & 0 & -q & -s \end{bmatrix}, \quad (22)$$

$$\Phi(x) = \begin{bmatrix} 0 \\ -\alpha(ax_1'^2 + \kappa x_1^2 - \gamma)x_1' - d(x_1' - x_3') \\ 0 \\ -\alpha(ax_2'^2 + \kappa x_2^2 - \gamma)x_2' - d(x_2' - x_3') \\ 0 \\ x_1 + x_2 - 2x_3 \end{bmatrix},$$

and $x = [x_1 \ x_1' \ x_2 \ x_2' \ x_3 \ x_3']^T$.

The next step is to determine the transformation that leads to the canonical form (3). Since for $\mu = 0$ system (21) becomes linear, such transformation can be easily obtained by diagonalizing A in the form $A = VDV^{-1}$, where D is a diagonal matrix containing the eigenvalues of A and V the matrix of corresponding eigenvectors, which are stored column-wise. For A as defined in Eq. (22), the diagonal matrix D verifies

$$D = \text{diag}(i, -i, i, -i, \sigma_1, \sigma_2), \quad (23)$$

where $\sigma_1 = \frac{1}{2}(-s + \sqrt{s^2 - 4q})$ and $\sigma_2 = \frac{1}{2}(-s - \sqrt{s^2 - 4q})$. Note that since $s > 0$ and $q > 0$, $\text{Re}(\sigma_1) < 0$ and $\text{Re}(\sigma_2) < 0$. Note further that $k=4$ and $l=6$ in Eq. (6).

By defining $x = Vy$, system (21) takes the canonical form, see Eq. (3)¹⁵

$$y' = Dy + \mu V^{-1}\Phi(Vy). \quad (24)$$

According to Eq. (7), the generating system (4) associated to Eq. (24) has solutions of the form

$$\begin{aligned} y_1 &= \alpha_1 e^{i\tau}, & y_2 &= \alpha_2 e^{-i\tau}, & y_3 &= \alpha_3 e^{i\tau}, & y_4 &= \alpha_4 e^{-i\tau}, \\ y_5 &= y_6 = 0. \end{aligned} \quad (25)$$

The amplitudes of these solutions are assumed to be complex,⁷ i.e., $\alpha_i = r_i e^{i\phi_i}$, $i = 1, 2, 3, 4$, where $\alpha_i \in \mathbb{C}$, $r_i \in \mathbb{R}_+$ and $\phi_i \in \mathcal{S}^1$. In this way, it is easy to analyze phase synchronization by looking at the phase differences. At this point, it is also worth noting that four eigenvalues of A appear in complex conjugate pairs, see Eq. (23). In order to have real solutions, it is necessary and sufficient that $\alpha_2 = \bar{\alpha}_1$ and $\alpha_4 = \bar{\alpha}_3$, i.e., $\phi_2 = -\phi_1$ and $\phi_4 = -\phi_3$ and correspondingly $r_1 = r_2$ and $r_3 = r_4$. This yields

$$\alpha_1 = r_1 e^{i\phi_1}, \quad \alpha_2 = r_1 e^{-i\phi_1}, \quad \alpha_3 = r_3 e^{i\phi_3}, \quad \alpha_4 = r_3 e^{-i\phi_3}. \quad (26)$$

In order to have a characterization for the synchronized regimen in terms of a single phase, the phase ϕ_3 is set to zero. Hence, synchronization is characterized by the phase $\phi = \phi_1$. Moreover, it will be assumed that the amplitudes are the same, i.e., $r = r_1 = r_3$ (compare this with Ref. 7). Consequently, the solutions (25) of the generating system become

$$\begin{aligned} y_1 &= r e^{i(\tau+\phi)}, & y_2 &= r e^{-i(\tau+\phi)}, & y_3 &= r e^{i\tau}, \\ y_4 &= r e^{-i\tau}, & y_5 &= y_6 = 0. \end{aligned} \quad (27)$$

Next, the values of r and ϕ are determined. This can be done by writing condition (8) of Theorem 1 as a system of equations in terms of r and ϕ . This yields

$$e^{i\phi} [\alpha(\gamma - (3a + \kappa)r^2) - d] - \frac{s(1 + e^{i\phi})}{(-1 + q)^2 + s^2} = 0, \quad (28)$$

$$\alpha(\gamma - (3a + \kappa)r^2) - d - \frac{f(s, \phi, q)}{(-1 + q)^2 + s^2} = 0, \quad (29)$$

$$\frac{i(1 - e^{-2i\phi})}{-1 + q - is} = 0, \quad (30)$$

where

$$f(s, \phi, q) = s + \frac{s}{2}(e^{i\phi} + e^{-i\phi}) + \frac{1}{2}(-1 + q)(e^{i\phi} + e^{-i\phi})i. \quad (31)$$

From Eq. (30), it follows that¹⁶

$$\phi = 0 \quad \text{or} \quad \phi = \pi. \quad (32)$$

The corresponding expressions for the half-amplitudes r of the periodic solutions are obtained by substitution of Eq. (32) into Eq. (28) or Eq. (29). This yields

- Existence: $\phi = 0$ (in-phase synchronization)

$$r = \sqrt{\frac{\gamma - \frac{(\sigma+d)}{\alpha}}{(3a + \kappa)}}, \quad (33)$$

with $\sigma = \frac{2s}{(-1+q)^2+s^2}$. Note that Eq. (33) is defined if $\gamma > \frac{\sigma+d}{\alpha}$.

- Existence: $\phi = \pi$ (anti-phase synchronization)

$$r = \sqrt{\frac{\gamma - \left(\frac{d}{\alpha}\right)}{(3a + \kappa)}}. \tag{34}$$

In this case, Eq. (34) will be defined if $\gamma > \frac{d}{\alpha}$.

Next, the local stability of the periodic solutions is investigated by using Eq. (11) in Theorem 1. This requires the computation of a characteristic polynomial for both the in-phase solution and the anti-phase solution.

- Local stability: $\phi = 0$ (in-phase synchronization)

After elaborated computations, one finds the following characteristic polynomial:

$$p_{in}(\chi) = [\chi + 2\pi(\alpha\gamma - d - \sigma)] \left[((1 - q)^2 + s^2)\chi^2 + 2\pi(\alpha\gamma - d - 2\sigma)\chi + c \right], \tag{35}$$

where

$$\sigma = \frac{2s}{(-1 + q)^2 + s^2}, \quad c = 4\pi^2(1 + s\sigma - s(\alpha\gamma - d)). \tag{36}$$

This polynomial will have roots with negative real part if and only if

$$C_1 = \gamma - \left(\frac{\sigma + d}{\alpha}\right) > 0, \quad C_2 = \gamma - \left(\frac{2\sigma + d}{\alpha}\right) > 0, \quad \text{and} \tag{37}$$

$$C_3 = -(\alpha\gamma - d) + \sigma + \frac{1}{s} > 0.$$

Note that condition $C_1 > 0$ is the same condition for the existence of the in-phase synchronous solution, see Eq. (33). Moreover, since $\sigma > 0$, condition $C_1 > 0$ is weaker than condition $C_2 > 0$. In other words, for Eq. (35) having negative roots, it is necessary and sufficient that $C_2 > 0$ and $C_3 > 0$.

By substituting the original parameters of Eqs. (15) and (16) in Eq. (37), it is possible to rewrite the conditions for C_2 and C_3 in terms of the original parameters including m_3 , i.e., the mass of the coupling bar. This yields

$$C_2 = 2H^* - \frac{8\beta_3\kappa^2 m}{\lambda[\kappa^2 m_3^2 - 2\kappa_3\kappa m m_3 + \kappa_3^2 m^2 + \beta_3^2 \kappa m]} - \frac{4\beta}{2\lambda m} > 0, \tag{38}$$

$$C_3 = -\frac{\lambda m_3}{\sqrt{\kappa m}} H^* + \frac{2m_3\beta_3}{\sqrt{\frac{\kappa}{m}} \left[m_3^2 - \frac{2\kappa_3 m m_3}{\kappa} + \frac{\kappa_3^3 m^2}{\kappa^2} + \frac{\beta_3^2 m}{\kappa} \right]} + \frac{\beta m_3}{m^{3/2}\sqrt{\kappa}} + \frac{\sqrt{\kappa m_3}}{\sqrt{m}\beta_3} > 0. \tag{39}$$

- Local stability: $\phi = \pi$ (anti-phase synchronization)

Again, after elaborated computations, one finds the following characteristic polynomial:

$$p_{anti}(\chi) = [\chi + 2\pi(\alpha\gamma - d)] \left[z\chi^2 + (2\pi z(\alpha\gamma - d)\chi + 4\pi^2(1 + s(\alpha\gamma - d))) \right], \tag{40}$$

where $z = (-1 + q)^2 + s^2$. In this case, the roots of $p_{anti}(\chi)$ will have negative real parts if and only if

$$C_4 = \gamma - \left(\frac{d}{\alpha}\right) > 0, \quad C_5 = \gamma - \left(\frac{d - \frac{1}{s}}{\alpha}\right) > 0. \tag{41}$$

Since d and s are positive, for $p_{anti}(\chi)$ having negative roots, it is sufficient that $C_4 > 0$. Note that, again, stability condition $C_4 > 0$ coincides with the condition for the existence of the solution, see Eq. (34).

Condition $C_4 > 0$ can be rewritten in terms of the original parameters of the system, i.e.,

$$C_4 = 2H^* - \frac{2\beta}{\lambda m} > 0. \tag{42}$$

Clearly, this condition for the existence and stability of the anti-phase regime does not depend on m_3 , i.e., the mass of the coupling bar. Note that this coincides with the fact that, ideally, the coupling bar comes to standstill when the oscillators synchronize in anti-phase, i.e., the coupling “disappears” during the anti-phase motion. Furthermore, it should be noted that condition (41) is “softer” than condition (37) for in-phase synchronization because if Eq. (37) is satisfied, then Eq. (41) will be satisfied too, whereas the opposite is not true.

Finally, the period of the synchronous solutions is computed. From Theorem 1 and Eq. (12), it follows that the in-phase synchronous solutions of system (21) have period

$$T_{in} = T + \tau_c(\mu) = 2\pi \left[1 + \frac{q - 1}{(-1 + q)^2 + s^2} \mu \right] + \mathcal{O}(\mu^2), \tag{43}$$

which is in terms of dimensionless time τ , whereas the anti-phase synchronous solutions will have dimensionless period

$$T_{anti} = T + \tau_c(\mu) = 2\pi + \mathcal{O}(\mu^2). \tag{44}$$

These results are very intuitive: when the oscillators synchronize in anti-phase, the coupling bar has no influence because it will be in rest and the oscillation frequency will closely approximate the eigenfrequency of the uncoupled, undamped oscillators. On the other hand, when the oscillators synchronize in-phase, the coupling bar converges to an oscillatory motion, which will influence the oscillation frequency of the oscillators.

The above results are summarized in the following two theorems and corollary.

Theorem 2. Consider system (19), (20). Assume $0 < \mu \ll 1$ and that the parameter values satisfy conditions (37). Then, in-phase synchronized solutions exist in system (19), (20) and these solutions are (asymptotically) stable, i.e.,

$$\lim_{t \rightarrow \infty} e_{in}(t) := x_1(t) - x_2(t) = 0, \tag{45}$$

$$\lim_{t \rightarrow \infty} \dot{e}_{in}(t) := \dot{x}_1(t) - \dot{x}_2(t) = 0.$$

Moreover, the in-phase limit solutions corresponding to the oscillators have amplitude

$$A_{in-phase}(\mu) = 2r = 2\sqrt{\frac{\gamma - \frac{(\sigma+d)}{\alpha}}{(3a + \kappa)}} = 2\sqrt{\frac{2H^* - \mu h_1 - \frac{4\zeta\omega}{\lambda}}{3m\omega^2 + \kappa}}, \quad (46)$$

with $h_1 = \frac{8\zeta_3\omega_3\omega^4}{\lambda[\omega^4 - 2\omega_3^2\omega^2 + \omega_3^4 + 4\zeta_3^2\omega_3^2\omega^2]}$ and period

$$T_{in-phase} = T + \tau_c(\mu) = 2\pi \left[1 + \frac{q-1}{(-1+q)^2 + s^2} \mu \right] + \mathcal{O}(\mu^2). \quad (47)$$

Theorem 3. Consider system (19), (20). Assume that $0 < \mu \ll 1$ and that the parameter values satisfy conditions (41). Then, anti-phase synchronized solutions exist and are (asymptotically) stable, i.e.,

$$\begin{aligned} \lim_{t \rightarrow \infty} e_{an}(t) &:= x_1(t) + x_2(t) = 0, \\ \lim_{t \rightarrow \infty} \dot{e}_{an}(t) &:= \dot{x}_1(t) + \dot{x}_2(t) = 0, \end{aligned} \quad (48)$$

and

$$\lim_{t \rightarrow \infty} x_3(t) = \dot{x}_3(t) = 0. \quad (49)$$

Moreover, the anti-phase limit solutions corresponding to the oscillators have amplitude

$$A_{anti-phase} = 2r = 2\sqrt{\frac{\gamma - \frac{d}{\alpha}}{(3a + \kappa)}} = 2\sqrt{\frac{2H^* - \frac{4\zeta\omega}{\lambda}}{3m\omega^2 + \kappa}} \quad (50)$$

and period

$$T_{anti-phase} = T + \tau_c(\mu) = 2\pi + \mathcal{O}(\mu^2). \quad (51)$$

Corollary 1. If $0 < \mu \ll 1$ and condition (37) is satisfied then system (19), (20) admits both in-phase and anti-phase synchronized solutions and both solutions are locally asymptotically stable.

Now, these analytical results are illustrated and supported by means of numerical simulations. Consider system (19), (20) with the following parameter values: $a = 37.1080$ [kg rad²/s²], $\gamma = 1.6 \times 10^{-3}$ [Nm], $\kappa = 37.1080$ [N/m], $\mu = \frac{2.1 \times 10^{-1}}{m_3}$ [-], $d = \frac{1.43 \times 10^{-2}}{m_3}$ [-], $\alpha = \frac{19.9}{m_3}$ [s²/(kg m² rad)], $q = 14.750\mu$ [-], and $s = 1.169\mu$ [-]. Some of these parameters have been chosen such that the limitations on damping and nonlinearities, see Sec. I, are satisfied. Other parameter values have been taken from a model corresponding to the experimental platform presented in Ref. 24 (see also Sec. V in this manuscript).

It follows that for the aforementioned values, conditions (37) are satisfied if $m_3 > 5.68$ [kg], see Figure 2. Here, a value of $m_3 = 16.8$ [kg] is considered. Consequently, $\mu = 0.0125$ [-].

Figure 3 shows the obtained simulation results. The nonzero initial conditions are $x_1(0) = 3 \times 10^{-3}$ [m], $x_2(0) = 2 \times 10^{-3}$ [m]. After initial transient behaviour, the oscillators synchronize in-phase, as depicted in Figure 3. By using Eq. (46), the limit amplitude of the synchronized solution is computed. It follows that for the given parameters $A_{in-phase} = 4.713 \times 10^{-3}$ [m]. This value and its negative counterpart are denoted by the horizontal dotted lines in Figure 3(b). The agreement between the analytical and the numerical results is evident. In fact, the difference between the actual amplitude and predicted amplitude is 2.256%. Additionally, the period of the synchronous solution is computed by using Eq. (47). This yields $T_{in-phase} = 6.1928$ [-]. Again, this result is very close (with an error of 0.033%) to the obtained result by numerical integration of Eqs. (19) and (20) as depicted in Figure 3(b) (vertical dotted lines). These differences are due to the fact that the theoretical analysis has been performed by using an approximated method and, moreover, high order terms in μ have been neglected. Additionally, since for the given parameter values also condition (41), see Theorem 3, holds with $C_4 = 8.487 \times 10^{-4}$, it follows that also stable anti-phase synchronization exists. This case is presented in Figures 3(c) and 3(d). These results have been obtained by using the same parameter values as above except for the initial condition of oscillator 2, which now is $x_2(0) = -5 \times 10^{-4}$ [m]. Clearly, the oscillators are synchronized in anti-phase. The amplitude of the anti-phase

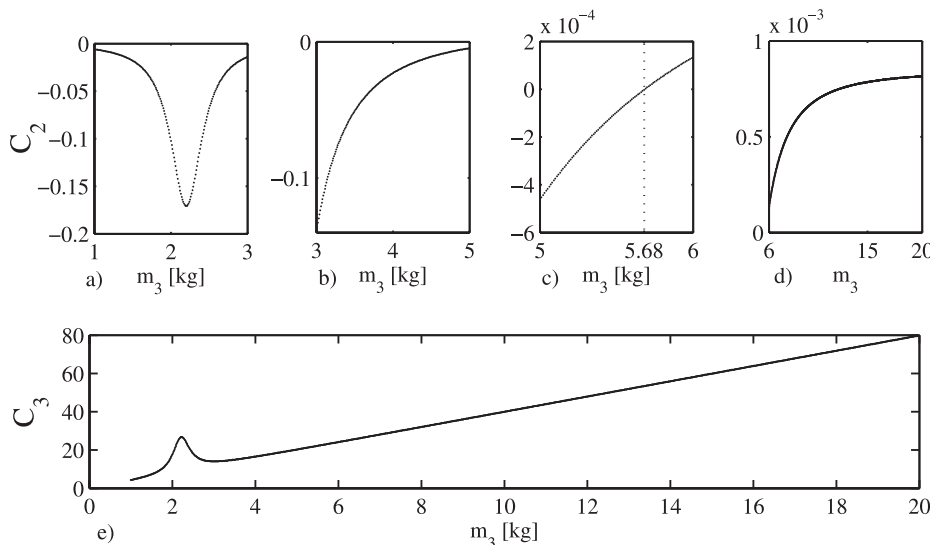


FIG. 2. Conditions (37) for in-phase synchronization plotted as a function of the mass of the coupling bar, i.e., m_3 . Figures 2(a) to 2(d): C_2 . Figure 2(e): C_3 .

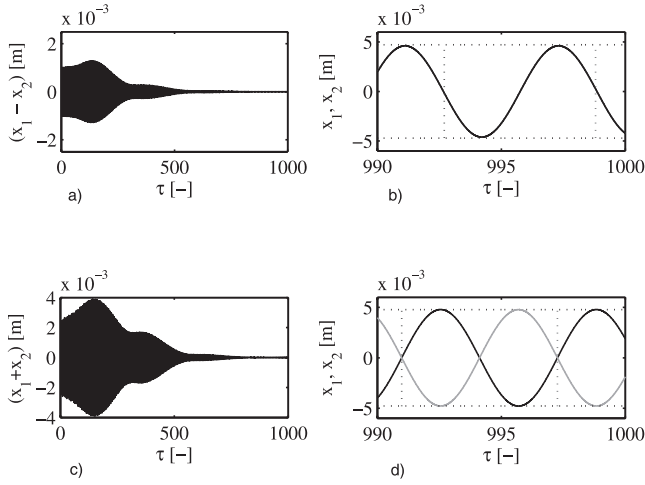


FIG. 3. For a small coupling strength (m_3 large) and initial conditions close to in-phase, system (19), (20) synchronizes in-phase as depicted in Figures 3(a) and 3(b). For the same coupling strength and initial conditions close to anti-phase, the oscillators synchronize in anti-phase, as shown in Figures 3(c) and 3(d), where black line: x_1 and grey line: x_2 .

solution, computed by using Eq. (50) in Theorem 3, is $A_{anti-phase} = 4.782 \times 10^{-3}$ [m]. Again, this value and its negative counterpart are indicated by two horizontal lines in Figure 3(d). The error in the predicted amplitude and the actual amplitude of the solution is 0.083%. The period of the solution, indicated by two vertical lines in Figure 3(d), is $T_{anti-phase} = 6.2827$ [-], whereas the expected value from Eq. (51) in Theorem 3 is $T = 2\pi$, i.e., there is a difference of 0.006%.

In order to illustrate the influence of the coupling strength $\mu = \frac{m}{m_3}$ in the limit synchronizing behaviour of the oscillators, system (19), (20) is again numerically integrated by using the same parameter values and initial conditions as used in the first simulation presented above, except for the coupling strength, which is increased by decreasing m_3 to $m_3 = 4.1$ [kg]. This yields $\mu = 0.0512$ [-]. Consequently, condition (37), see Theorem 2, is not fulfilled. However, condition (41), see Theorem 3, is satisfied and consequently the only stable solution is anti-phase synchronization, as depicted in Figure 4. It can be seen that although the initial conditions of the system are very close to in-phase motion, after initial transient behaviour, the system synchronizes in anti-phase.

IV. SYNCHRONIZATION OF OSCILLATORS DRIVEN BY A VAN DER POL TERM

A classical (circuit) model of a nonlinear oscillator showing a self-sustained oscillation is due to van der Pol.²⁶ The key feature in the model is the presence of a nonlinear damping term, which dissipates energy for large amplitudes—acting like ordinary positive damping—and generates energy at low amplitudes—acting like negative damping. It should be noticed that this term has more or less the same effect as an escapement mechanism in a pendulum clock: energy is delivered to the system such that the oscillations do not damp out. Consequently, it is not surprising that there exist several works related to the classical Huygens system where the escapement mechanism has been modelled

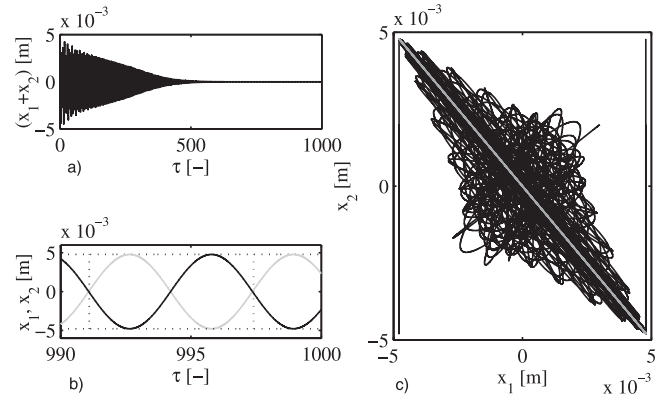


FIG. 4. When the coupling strength is increased (by decreasing m_3) the only synchronous solution in system (19), (20) is anti-phase synchronization. In Fig. 4(b), black line: x_1 and grey line: x_2 . In Fig. 4(c), black line: transient behaviour and grey: long term behaviour.

by using the nonlinear damping term of the van der Pol equation, see, e.g., Refs. 5, 22, and 31. This facilitates the modelling of the real escapement mechanism and allows to perform a fairly complete analytic analysis of the in-phase and anti-phase synchronized motion, which becomes tremendously involved if the escapement is modelled, for instance, by an impulsive function.^{9,27}

This section investigates the occurrence of synchronization in the system of coupled oscillators depicted in Figure 1(b) for the case where the resupply of energy into the oscillators is provided by the van der Pol term

$$U_i = -\eta(ax_i^2 - 1)\dot{x}_i, \quad i = 1, 2, \quad (52)$$

where $\eta \in \mathbb{R}_+$ determines the amount of nonlinearity and the strength of the damping and $a \in \mathbb{R}_+$ is a parameter, which defines the switching between positive and negative damping. For $x_i < \frac{1}{\sqrt{a}}$, the velocity in oscillator i is increased and for $x_i > \frac{1}{\sqrt{a}}$, it is decreased.

By again assuming identical oscillators, it can be shown that the dynamic behaviour of the coupled system shown in Figure 1(b) with input (52) is described by

$$\ddot{x}_i = -\omega^2(x_i - x_3) - 2\zeta\omega(\dot{x}_i - \dot{x}_3) - \nu(ax_i^2 - 1)\dot{x}_i \quad i = 1, 2, \quad (53)$$

$$\ddot{x}_3 = -\omega_3^2 x_3 - 2\zeta_3 \omega_3 \dot{x}_3 - \mu \sum_{i=1}^2 \ddot{x}_i, \quad (54)$$

where as defined in Sec. III, $\omega, \omega_3, \zeta, \zeta_3$ are positive parameters, $\nu = \frac{\mu}{m} \in \mathbb{R}_+$, and μ is the coupling strength.

System (53), (54) resembles a pair of van der Pol oscillators with Huygens' coupling. In order to derive conditions for the onset of in-phase and anti-phase synchronized motion in the coupled system (53), (54), the analytical method presented in Sec. II is used again. This again requires to transform the system into the form (3). By setting $\tau = \omega t$, $p = 2\zeta$, $q = \frac{\omega_3^2}{\omega^2}$, $s = \frac{2\zeta_3 \omega_3}{\omega}$, and $\bar{\lambda} = \frac{\nu}{\omega}$, and assuming that the damping in the oscillators and, therefore, the amplitude of the nonlinear van der Pol term are small, i.e., $p = \mu d$ and $\bar{\lambda} = \mu \alpha$, it is possible to rewrite Eqs. (53) and (54) in the form

$$x' = Ax + \mu\Phi_1(x) + \mu^2\Phi_2(x), \tag{55}$$

where the prime denotes differentiation with respect to the dimensionless time $\tau = \omega t$, and $x = [x_1 \ x'_1 \ x_2 \ x'_2 \ x_3 \ x'_3]^T$ is the state vector, A is as given by Eq. (22), and

$$\Phi_1 = \begin{bmatrix} 0 \\ -d(x'_1 - x'_3) - \alpha(ax_1^2 - 1)x'_1 \\ 0 \\ -d(x'_2 - x'_3) - \alpha(ax_2^2 - 1)x'_2 \\ 0 \\ x_1 + x_2 - 2x_3 \end{bmatrix}, \tag{56}$$

$$\Phi_2 = \begin{bmatrix} 0 \\ 0 \\ 0 \\ 0 \\ 0 \\ \sum_{i=1}^2 (dx'_i + \alpha(ax_i^2 - 1)x'_i) - 2dx'_3 \end{bmatrix}.$$

By following a similar approach as presented in Sec. III, it is possible to show that the following results for system (55), (56) hold.

Theorem 4. Consider system (55), (56). Assume $0 < \mu \ll 1$ and that the parameter values satisfy the following conditions:

$$C_1 = 1 - \left(\frac{2\sigma + d}{\alpha}\right) > 0, \text{ and } C_2 = -1 + \left(\frac{\sigma + d + \frac{1}{s}}{\alpha}\right) > 0, \tag{57}$$

where σ is defined by Eq. (36). Then, in-phase synchronized solutions exist in system (55) and these solutions are (asymptotically) stable, i.e.,

$$\lim_{t \rightarrow \infty} e_{in}(t) := x_1(t) - x_2(t) = 0, \quad \lim_{t \rightarrow \infty} \dot{e}_{in}(t) := \dot{x}_1(t) - \dot{x}_2(t) = 0. \tag{58}$$

Moreover, the in-phase limit solutions corresponding to the oscillators have amplitude

$$A_{in-phase}(\mu) = 2r = 2\sqrt{\frac{\alpha - (\sigma + d)}{\alpha}} = 2\sqrt{\frac{1 - \mu h_1 - \frac{2\zeta\omega}{\nu}}{a}}, \tag{59}$$

with $h_1 = \frac{4\zeta_3^2\omega_3^4}{\lambda[\omega^4 - 2\omega_3^2\omega^2 + \omega_3^4 + 4\zeta_3^2\omega_3^2\omega^2]}$, and period

$$T_{in-phase} = T + \tau_c(\mu) = 2\pi \left[1 + \frac{q - 1}{(-1 + q)^2 + s^2} \mu \right] + \mathcal{O}(\mu^2). \tag{60}$$

Theorem 5. Consider system (55), (56). Assume $0 < \mu \ll 1$ and that the following condition holds:

$$\alpha - d > 0. \tag{61}$$

Then, anti-phase synchronized solutions exist and are (asymptotically) stable, i.e.,

$$\lim_{t \rightarrow \infty} e_{an}(t) := x_1(t) + x_2(t) = 0, \quad \lim_{t \rightarrow \infty} \dot{e}_{an}(t) := \dot{x}_1(t) + \dot{x}_2(t) = 0 \tag{62}$$

and

$$\lim_{t \rightarrow \infty} x_3(t) = \dot{x}_3(t) = 0. \tag{63}$$

Moreover, the anti-phase limit solutions corresponding to the oscillators have amplitude

$$A_{anti-phase} = 2r = 2\sqrt{\frac{1 - \frac{d}{\alpha}}{a}} = 2\sqrt{\frac{1 - \frac{2\zeta\omega}{\nu}}{a}} \tag{64}$$

and period

$$T_{anti-phase} = T + \tau_c(\mu) = 2\pi + \mathcal{O}(\mu^2). \tag{65}$$

Note that condition (61) is weaker than condition (57). Hence, when Eq. (57) is satisfied, both in-phase and anti-phase synchronous solutions exist and are locally asymptotically stable. On the other hand, when Eq. (61) is satisfied and condition (57) is not satisfied, then the only stable synchronous solution is anti-phase synchronization. By means of numerical integration, it is possible to show countless examples.

V. EXPERIMENTAL RESULTS

The obtained results in Secs. III and IV have been derived under the assumption that the oscillators are identical. Obviously, in a real physical system, it is impossible to have two identical oscillators. A mathematical treatment, in which external perturbations (like noise) and unmodelled dynamics are taken into account, turns out to be complicated and the available mathematical tools are limited. Therefore, in this section, an experimental analysis is performed in order to get insight into the existence of synchronization in a real system where there are unavoidable small mismatches/disturbances in the oscillators. The analysis is conducted by using the electro-mechanical setup depicted in Figure 5, which is schematically depicted in Figure 1(b). It consists of two actuated oscillators mounted on an (actuated) elastically supported rigid bar. The system has 3 dofs corresponding to the horizontal displacements of the two oscillators and the bar, respectively.

Since the oscillators are actuated separately, then via computer-controlled feedback it is possible to mimic a variety of different controlled/uncontrolled synchronizing systems. In fact, the purpose of the control inputs U_1 and U_2 (see Figure 1(b)) is twofold: to guarantee self-sustained oscillations and to modify the inherent dynamic properties of the oscillators, such as mass, stiffness, and damping properties, in a desired way. For a detailed description of the setup, the interested reader is referred to Ref. 24.

A. Energy-dependent escapement

In a first set of experiments, the inherent mechanical properties of the experimental setup of Figure 5 are adjusted

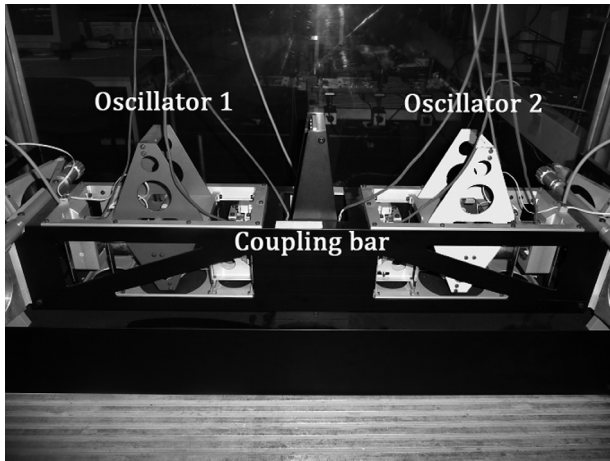


FIG. 5. Photo of the experimental setup.

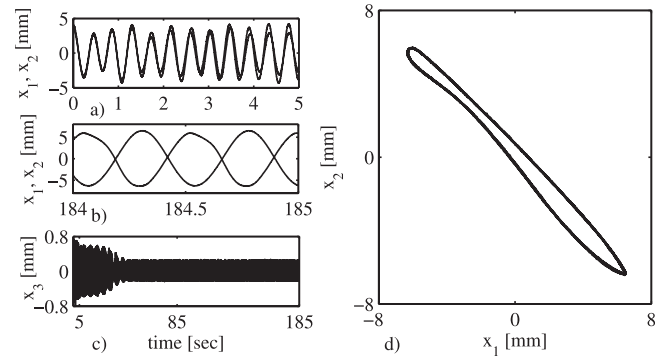
such that its dynamic behaviour is described by the set of equations (19) and (20). The parameter values for the experiments are given in Table I. For the experiments, all parameter values and initial conditions are fixed and the only parameter that is modified from experiment to experiment is m_3 , the mass of the coupling bar, which influences the coupling strength $\mu = \frac{m}{m_3}$. The nonzero initial conditions are $x_1(0) = 4$ [mm], $x_2(0) = 3.5$ [mm]. Note that in the experiment the intention still is to make the oscillators identical but it should be noted that it will be practically impossible to realize this.

In a first experiment, the mass of the coupling bar is $m_3 = 4.1$ [kg] and, consequently, $\mu = 0.0512$ [–]. For the given parameter values, condition (41), see Theorem 3, is satisfied, whereas condition (37), see Theorem 2, is not fulfilled.¹⁷ Hence, anti-phase synchronization is expected to occur in this experiment.

Figure 6 summarizes the main results. Although the oscillators are released close to in-phase, as depicted in Figure 6(a), after initial transient behaviour, the oscillators *practically* synchronize in anti-phase, as shown in Figures 6(b) and 6(d). Although initially the oscillations in the coupling bar are large due to the nearly in-phase start-up, in the limit, when the oscillators practically synchronize in anti-phase, the amplitude of the oscillations (in the motion) of the coupling bar becomes relatively small as depicted in Figure 6(c). Ideally, for identical oscillators, the oscillations in the coupling bar should decay to zero. However, in the experiment, the oscillators are not identical as can be seen from

TABLE I. Parameter values for the energy-dependent escapement experiments.

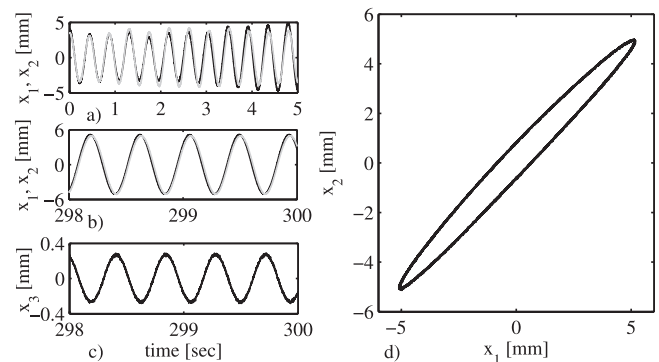
Oscillator 1,2	Coupling bar
$m = 2.10 \times 10^{-1}$ [kg]	$m_3 \in \{4.1, 15.95\}$ [kg]
$\kappa = 37.108$ [N/m]	$\kappa_3 = 3.8871 \times 10^2$ [N/m]
$\beta = 5 \times 10^{-2}$ [Ns/m]	$\beta_3 = 3.2656$ [Ns/m]
$d = 8.52 \times 10^{-2} m_3$ [–]	...
$\alpha = 106.71 m_3$ [–]	...
$a = 37.108$ [–]	...
$\gamma = 1.567 \times 10^{-3}$ [–]	...

FIG. 6. Experimental results. For relatively large coupling strength, the oscillators practically synchronize in anti-phase. In Figures 6(a) and 6(b), black line: x_1 and grey line: x_2 . Figure 6(d) does not contain transient behaviour.

Figures 6(b) and 6(d). Roughly speaking, the “pushing force” of one oscillator exerted to the coupling bar is larger than the “pulling force” exerted by the other oscillator and, consequently, the coupling bar does not come to a complete standstill.

In a second experiment, the mass of the coupling bar is increased by adding five steel plates with a mass of approximately 2.370 [kg] each. This yields $m_3 \approx 15.95$ [kg], i.e., $\mu = 0.0131$ [–]. The remaining parameter values and initial conditions are the same as used in the previous experiment. Note that in this case, condition (37) in Theorem 2 is satisfied. As a consequence of adding mass to the coupling bar, the oscillators now *practically* synchronize in-phase as shown in Figure 7. The coupling bar converges to an oscillatory motion with fixed amplitude and frequency, as shown in Figure 7(c). Moreover, the frequency of the in-phase synchronous solution of the oscillators is very close to ω_3 . The amplitude of the vibrations in the coupling bar is of the same order in Figures 6 and 7. Note, however, that the mass of the coupling bar is about four times higher in Figure 7.

In both experiments, the amplitudes and frequencies of the synchronous solutions differ from the analytical values given by Theorems 2 and 3, respectively. For instance, in case of the first experiment, the amplitude of the anti-phase synchronous solution is 6.47 [mm] for the first oscillator and 6.31 [mm] for the second one. If the parameter values used

FIG. 7. In this experiment, the mass of the coupling bar is increased to $m_3 = 15.95$ [kg] (coupling strength is decreased). As a consequence, the oscillators practically synchronize in-phase. In Figures 7(a) and 7(b), black line: x_1 and grey line: x_2 . Figure 7(d) does not contain transient behaviour.

during the experiment are substituted in Eq. (50), then the expected amplitude is 4.551 [mm]. Regarding the frequency of the synchronous solution, the same experiment reveals that the oscillators synchronize in anti-phase with a frequency of 2.1155 Hz, i.e., $T=0.4727$ [s], whereas Eq. (51) in Theorem 3 yields $T=0.4726$ [s] (converting dimensionless time τ back to the real time t). For the second experiment, the amplitude of the oscillations in oscillator 1 is 5.166 [mm] and 4.939 [mm] for the second oscillator, whereas the predicted amplitude from Theorem 2 is 4.479 [mm]. The frequency of the in-phase synchronous solution in the experiment is $T=0.4342$ [s], whereas the predicted period from Theorem 2 is $T=0.4654$ [s]. These differences should not be surprising since, as has been mentioned before, the oscillators in the experimental setup are not identical and the theoretical results summarized in Theorems 2 and 3 have been derived under the assumption of identical oscillators. Moreover, the theoretical analysis has been conducted for the nonlinear system in an approximated form.

B. van der Pol escapement

Similar experiments have been conducted for the case where the experimental setup is adjusted to mimic the dynamics (in terms of the time t) of the coupled system (55) analyzed in Sec. IV. The parameter values for the experiments are provided in Table II. For the experiments, all parameter values and initial conditions are fixed and the only parameter that is modified from experiment to experiment is m_3 , the mass of the coupling bar, which influences the coupling strength $\mu = \frac{m}{m_3}$. The nonzero initial conditions are $x_1(0) = 3$ [mm] and $x_2(0) = 2.8$ [mm].

Again, in the first experiment, a light coupling bar, i.e., $m_3 = 4.1$ [kg], i.e., $\mu = 0.0512$ [–], is used. For the given parameter values, condition (61) in Theorem 5 is satisfied, whereas condition (57) in Theorem 4 is not fulfilled,¹⁸ Hence, for this experiment, anti-phase synchronization is expected to occur.

As becomes clear from Figures 8(b) and 8(d), indeed the oscillators practically synchronize in anti-phase, although they were released close to in-phase synchronization as depicted in Figure 8(a). The behaviour of the coupling bar is depicted in Figure 8(c). Initially, the transient part of the displacement of the bar is relatively large due to the nearly in-phase startup of the oscillators. Later, when the phase difference between the oscillators tends to π [rad], the amplitude of the oscillations in the bar reduces to a small value. In the experiment, the amplitude of the oscillations is 7.776

TABLE II. Parameter values for the van der Pol escapement experiments.

Oscillator 1,2	Coupling bar
$m = 2.10 \times 10^{-1}$ [kg]	$m_3 \in \{4.1, 15.95\}$ [kg]
$\kappa = 37.108$ [N/m]	$\kappa_3 = 3.8871 \times 10^2$ [N/m]
$\beta = 8 \times 10^{-3}$ [Ns/m]	$\beta_3 = 3.2656$ [Ns/m]
$d = 1.36 \times 10^{-2} m_3$ [–]	...
$\alpha = 3.58 \times 10^{-2} m_3$ [–]	...
$a = 1 \times 10^5$ [1/m ²]	...

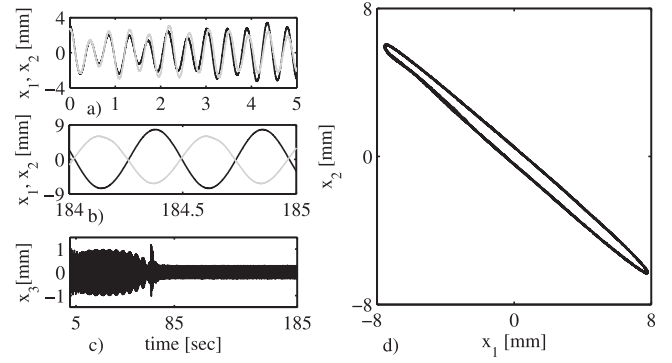


FIG. 8. Experimental results. For a light coupling bar $m_3 = 4.1$ [kg] (relatively large coupling strength μ), practical anti-phase synchronization occurs. In Figures 8(a) and 8(b), black line: x_1 and grey line: x_2 . In Figure 8(d), transient behaviour has been omitted.

[mm] for the first oscillator and 6.09 [mm] for the second oscillator. Furthermore, the period of the synchronous solution is $T=0.4729$ [s]. The amplitude and period of the synchronous solution when computed by using Eqs. (64) and (65) are 4.976 [mm] and 0.4726 [s], respectively.

In a second experiment, the mass of the coupling bar is increased by adding ten steel plates of approximately 2.370 [kg] each. This yields $m_3 \approx 27.8$ [kg], i.e., $\mu = 0.0075$ [–]. The remaining parameters and initial conditions are the same as used in the previous experiment. Note that in this case, condition (57) in Theorem 4 is satisfied. In fact, as a consequence of adding mass to the coupling bar, the oscillators practically synchronize in-phase as depicted in Figure 9. The motion of the coupling bar converges to an oscillatory motion with fixed amplitude and frequency, as shown in Figure 9(c). Moreover, the frequency of the in-phase synchronous solution is very close to the frequency of the coupling bar. The oscillations in the first oscillator have amplitude 5.871 [mm], whereas for the second oscillator the amplitude of the oscillations is 5.603 [mm]. The in-phase synchronous solution has period $T=0.4340$ [s]. For the given parameter values, Theorem 4 predicts a synchronous solution with amplitude equal to 4.891 [mm] and period $T=0.4687$ [s].

Finally, in order to illustrate the influence of the initial conditions in the limit synchronizing behaviour of the

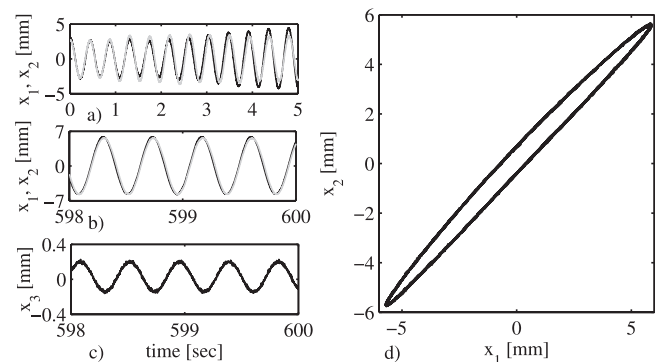


FIG. 9. In this experiment, the oscillators practically synchronize in-phase. The oscillators have been released from initial conditions close to in-phase and the mass of the coupling bar has been increased to $m_3 = 27.8$ [kg]. In Figures 9(a) and 9(b), black line: x_1 and grey line: x_2 . In Figure 9(d), transient behaviour has been omitted.

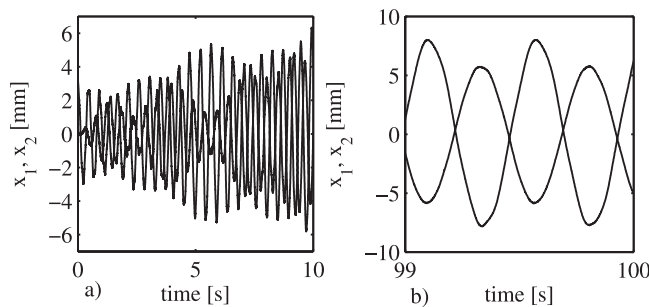


FIG. 10. For initial conditions far from in-phase, the oscillators synchronize in anti-phase. Black line: x_1 and grey line: x_2 .

system, experiment 2 is repeated by only changing the initial condition of oscillator 2, which now is $x_2(0) = 0$ [rad]. As can be seen in Figure 10, the oscillators now synchronize in anti-phase.

Summarizing, the experimental results qualitatively agree with the analytical results. Quantitative differences, as explained before, originate from the fact that in the real physical system the oscillators are not identical and original dynamics of the setup cannot be completely cancelled. Moreover, Theorems 2 to 5 are used in an approximated form (higher order terms are neglected). Nevertheless, analytical results and experimental results convey the same message: the mass of the coupling bar m_3 (or the coupling strength μ) influences the limit synchronizing behaviour in the oscillators.

Note that the results obtained here are largely in agreement with other experimental results available in the literature. Consider for example the system described in Ref. 20. It consists of two metronomes attached to a bar that can move horizontally. The authors observed that anti-phase synchronization was the “dominant” synchronous solution. Moreover, the authors mention that in-phase synchronization was observed only when the mass of the bar was increased. Likewise, in Ref. 22, where the setup consists of a pair of metronomes placed on a freely moving rigid bar, which rests on top of two soda cans, the author explains that anti-phase synchronization was observed only when the coupling strength was increased.

VI. DISCUSSION

The occurrence of synchronized motion in pairs of weakly nonlinear oscillators interacting via Huygens’ coupling has been investigated. Sufficient conditions for the existence and local stability of synchronous solutions have been derived using the Poincaré method based on a small parameter. For the present case, this “small parameter” appears naturally in the system and corresponds to the coupling strength μ , i.e., the ratio between the oscillators’ mass m and the mass of the coupling bar m_3 .¹⁹

The analysis has revealed that the mass of the coupling bar (or the coupling strength) influences the limit synchronized behaviour in the system, namely anti-phase or in-phase synchronization. Decreasing the coupling strength, i.e., increasing the mass of the coupling bar, facilitates the onset of in-phase synchronization. On the other hand, when the coupling strength is increased, i.e., by decreasing the mass of

the coupling bar, anti-phase synchronization is the only expected stable synchronous mode.

Moreover, Corollary 1 establishes that by decreasing the coupling strength μ , it is possible to have two coexisting types of stable synchronous motion: in-phase and anti-phase. Consequently, the limit behaviour in this case is determined by the initial conditions. Computer simulations have revealed that when the oscillators are released close to in-phase then the limit behaviour of the system will be in-phase synchronization, whereas for the remaining initial conditions the limit behaviour is anti-phase synchronization, i.e., the region of attraction for anti-phase is larger than the attraction region for in-phase.

Additionally, the onset of synchronization in two oscillators with Huygens’ coupling has been investigated in a real system, i.e., by means of experiments. In fact, the experiments have confirmed that a light coupling bar yields anti-phase synchronous motion in the oscillators, whereas with a heavier coupling bar in-phase synchronization can be observed.

In conclusion, if the reader reflects on the results presented in this manuscript the following must be clear: the synchronization phenomenon observed by Huygens more than 300 years ago in a pair of pendulum clocks can also be observed if the pendulums are replaced by other oscillators.

ACKNOWLEDGMENTS

This research was (partly) supported by the Mexican Council for Science and Technology, CONACYT.

¹Oxford Advanced Learner’s Dictionary (Oxford University Press, Oxford, 1997).

²A. A. Andronov, A. A. Vitt, and S. E. Khaikin, *Theory of Oscillators* (Dover Publications, New York, 1987).

³M. Bennett, M. Schatz, H. Rockwood, and K. Wiesenfeld, “Huygens’ clocks,” *Proc. R. Soc. London, Ser. A* **458**, 563–579 (2002).

⁴I. I. Blekhan, *Synchronization of Dynamic Systems* (Nauka, Moscow, 1971).

⁵I. I. Blekhan, *Synchronization in Science and Technology* (ASME Press, New York, 1988).

⁶C. Huygens, in *Oeuvres complètes de Christiaan Huygens*, edited by M. Nijhoff (J. Enschedé & Fils, The Hague, 1932), Vol. 17, pp. 156–189.

⁷V. Jovanovic and S. Koshkin, “Synchronization of Huygens’ clocks and the Poincaré method,” *J. Sound Vib.* **331**, 2887–2900 (2012).

⁸I. G. Malkin, *Some Problems in the Theory of Nonlinear Oscillations* (State Publishing House of Technical and Theoretical Literature, Moscow, 1956).

⁹F. C. Moon, “Chaotic clocks: A paradigm for the evolution of noise in machines,” in *IUTAM Symposium*, edited by G. Rega and F. Vestroni (Springer, London, 2005).

¹⁰A. H. Nayfeh and D. T. Mook, *Nonlinear Oscillations* (John Wiley & Sons, New York, 1979).

¹¹H. Nijmeijer, I. Blekhan, A. Fradkov, and A. Pogromski, “Self-synchronization and controlled synchronization,” in *Proceedings of the First International Conference on Control of Oscillations and Chaos*, St. Petersburg, Russia, 27–29 August 1997, pp. 36–41.

¹²Because μ is considered to be small, system (1) is often called *quasilinear* system.

¹³However, it is required that the algebraic multiplicity of these roots is equal to their geometric multiplicity.

¹⁴An abbreviated notation is used for the determinant of a $n \times n$ matrix with components a_{sj} as $|a_{sj}|$, $s, j = 1, \dots, n$. The symbol δ_{sj} is the Kronecker delta.

¹⁵Note that this transformation is valid since the matrix of eigenvectors associated to Eq. (23) has full rank. Eigenvalue i as well as eigenvalue $-i$ have geometric and algebraic multiplicity equal to 2.

¹⁶Actually, Eq. (30) is satisfied for $\phi = \pm n\pi$ with $n = 0, 1, 2, \dots$

¹⁷For the given parameters, condition (37) is satisfied if $m_3 > 6.1267$ [kg].

- ¹⁸For the given parameters, condition (57) in Theorem 4 is satisfied if $m_3 > 8.8519$ [kg].
- ¹⁹Clearly, the coupling strength may be affected by modifying m and/or m_3 . However, modifying m requires to modify the dynamics of the uncoupled oscillators, which is not intended in the present study. Hence, in the analysis presented in this paper, the coupling strength has been modified by means of the mass of the coupling bar m_3 .
- ²⁰W. T. Oud, H. Nijmeijer, and A. Y. Pogromsky, "A study of Huygens' synchronization: Experimental results," in *Group Coordination and Cooperative Control, Lecture Notes in Control and Information Sciences Vol. 336*, edited by K. Pettersen, J. Gravdahl, and H. Nijmeijer (Springer, Berlin, 2006), pp. 191–203.
- ²¹E. V. Pankratova and V. N. Belikh, "Synchronization of self-sustained oscillators inertially coupled through common damped system," *Phys. Lett. A* **376**, 3076–3084 (2012).
- ²²J. Pantaleone, "Synchronization of metronomes," *Am. J. Phys.* **70**, 992–1000 (2002).
- ²³J. Pena-Ramirez, "Huygens' synchronization of dynamical systems," Ph.D. thesis (Eindhoven University of Technology, 2013).
- ²⁴J. Pena-Ramirez, R. H. B. Fey, and H. Nijmeijer, "An experimental study on synchronization of nonlinear oscillators with Huygens' coupling," *NOLTA, IEICE* **3**, 128–142 (2012).
- ²⁵A. Pikovsky, M. Rosenblum, and J. Kurths, *Synchronization. A Universal Concept in Nonlinear Sciences* (Cambridge University Press, Cambridge, 2001).
- ²⁶B. van der Pol, "On relaxation-oscillations," *Philos. Mag. Ser. 7* **2**, 978–992 (1926).
- ²⁷A. V. Roup, D. S. Bernstein, S. G. Nersesov, W. S. Haddad, and V. Chellaboina, "Limit cycle analysis of the verge and foliot clock escapement using impulsive differential equations and Poincaré maps," *Int. J. Control* **76**, 1685–1698 (2003).
- ²⁸M. Senator, "Synchronization of two coupled escapement-driven pendulum clocks," *J. Sound Vib.* **291**, 566–603 (2006).
- ²⁹S. Strogatz, *Sync. The Emerging Science of Spontaneous Order* (Hyperion, New York, 2003).
- ³⁰S. Strogatz and I. Steward, "Coupled oscillators and biological synchronization," *Sci. Am.* **269**, 102–109 (1993).
- ³¹H. Ulrichs, A. Mann, and U. Parlitz, "Synchronization and chaotic dynamics of coupled mechanical metronomes," *Chaos* **19**, 043120-1–043120-6 (2009).
- ³²F. Verhulst, *Nonlinear Differential Equations and Dynamical Systems* (Springer-Verlag, Heidelberg, 1990).
- ³³K. Wiesenfeld and D. Borrero-Echeverry, "Huygens (and others) revisited," *Chaos* **21**, 047515 (2011).